

---

## End-To-End Timing Analysis in ROS2

Harun Teper, Mario Günzel, Niklas Ueter, Georg von der Brüggen, Jian-Jia Chen  
TU Dortmund University, Department of Computer Science, Dortmund, Germany

Citation:

---

### BIB<sub>T</sub>E<sub>X</sub>:

```
@inproceedings{22RTSS_TeperGUBC,  
  author={Harun Teper, Mario Günzel, Niklas Ueter, Georg von der Brüggen, Jian-Jia Chen},  
  booktitle={43rd IEEE Real-Time Systems Symposium (RTSS)},  
  title={End-To-End Timing Analysis in ROS2},  
  year={2022},  
  volume={},  
  number={},  
  pages={},  
  doi={}  
}
```

©2022 IEEE. Personal use of this material is permitted. Permission from IEEE must be obtained for all other uses, in any current or future media, including reprinting/republishing this material for advertising or promotional purposes, creating new collective works, for resale or redistribution to servers or lists, or reuse of any copyrighted component of this work in other works.

# End-To-End Timing Analysis in ROS2

Harun Teper, Mario Günzel, Niklas Ueter, Georg von der Brüggen and Jian-Jia Chen  
TU Dortmund University, Germany

{harun.teper, mario.guenzel, niklas.ueter, georg.von-der-brueggen, jian-jia.chen}@tu-dortmund.de



**Abstract**—Modern autonomous vehicle platforms feature many interacting components and sensors, which add to the system complexity and affect their performance. A key aspect for such platforms are end-to-end timing guarantees, which are required for safe and predictable behavior in every situation.

One widely used tool to develop such autonomous systems is the Robot Operating System 2 (ROS2), which allows creating robot applications composed of several components that communicate with each other to form complex systems. Furthermore, it guarantees real-time constraints and provides reliable timing behavior using a custom scheduler design that manages the execution of all components. These components and their data propagation form multiple cause-effect chains that can be analyzed to determine two key metrics: maximum reaction time (which is the maximum time for the system to react to an external input) and maximum data age (which equals the maximum time between sampling and the output of the system being based on that sample). However, an end-to-end analysis for cause-effect chains in ROS2 systems has not been provided yet.

In this paper, we provide a theoretical upper bound for the end-to-end timing of a ROS2 system on a single electronic control unit (ECU). Additionally, we show how to simulate a ROS2 system to get a lower bound for the timing analysis and introduce an online end-to-end timing measurement method for existing ROS2 systems. We evaluate our methods with a basic autonomous navigation system and determine the timing behavior for different components and sensor configurations.

**Index Terms**—End-to-End Timing, Maximum Reaction Time, Maximum Data Age, Robot Operating System 2

## I. INTRODUCTION

Modern autonomous vehicles include an increasing number of components, which must comply with timing constraints to ensure correct functionality and safety of both the vehicle and its environment. They include components like smart lights, ACC, and ABS on different electronic control units (ECU) that interact over an intra-vehicle network. Additionally, there are many system designs that feature different hardware and software solutions. As the complexity of these systems increases, guaranteeing timing constraints becomes more difficult.

One widely used software framework to develop autonomous systems is the Robot Operating System 2 (ROS2) [13], which is a set of software libraries and tools to develop robot software. ROS2 allows freely creating arbitrarily complex robot systems, as it provides tools to create simple components that can communicate with each other. It also provides a customizable scheduler abstraction, called an *executor*, which processes the time-triggered and event-triggered functions of each system component. The autonomous driving project Autoware.Auto [11], [19] represents one advanced open-source solution that is based on ROS2 and features autonomous valet-parking and cargo delivery.

One promise of ROS2 is the possibility of providing real-time guarantees, which was not considered in the original Robot Operating System (ROS) [15]. The ROS2 executor has been recently analyzed and optimized [2]–[5], [18]. Specifically, the execution of ROS2 components can be modeled as a directed acyclic graph (DAG), whose worst-case response time can be derived by extending existing timing analysis methods in real-time systems [2], [4]. Moreover, Choi et al. [5] proposed a priority assignment approach for the ROS2 executor to improve the worst-case response time. Instead of modeling the ROS2 components as a DAG, Tang et al. [18] proposed to model them as processing chains to perform worst-case response time analysis and optimize the component priorities.

If all components actively trigger the components they are connected to, then the communication between ROS2 components can be described by the worst-case response time of the DAG [2], [4], [5]. However, ROS2 also features components where the data propagation and execution order are independent from other tasks. For example, a chain of tasks can include multiple intermediate timers that are sporadically executed according to their period, or include a chain whose tasks are also triggered by tasks of other chains. Such chains can in fact be more properly modeled as a cause-effect chain.

A cause-effect chain models a sequence of reactions from the cause (e.g., sensing) to an effect (e.g., actuation). The definition of cause-effect chains for a ROS 2 system is inspired by the event-chains of the AUTOSAR Timing Extensions [1], as well as the definition of cause-effect chains by Günzel et al. [10] for periodic and sporadic task systems. Two types of end-to-end latencies are of most interest in the literature: the maximum reaction time (which is the maximum time for an external event to be processed by the system), and the maximum data age (which is the maximum duration between sampling and the output being based on that sample).

However, existing timing analyses for cause-effect chains, e.g., [6], [7], [10], [12], are only valid for periodic and sporadic task systems and cannot be directly applied to the event-triggered and time-triggered components of ROS2.

**Contributions:** We provide, to the best of our knowledge, the first end-to-end timing analysis for ROS2 cause-effect chains. We assume that our system has one ECU, whose components are scheduled by one single-threaded ROS2 executor. We detail the ROS2 architecture in Section II and introduce the task model, cause-effect chains, and analyzed timing values in Section III. Related work and a delimitation and discussion are presented in Sections IV and V, respectively.

This paper provides the following contributions:

- Section VI provides an upper bound analysis for the end-to-end latency of cause-effect chains in ROS2 systems.
- In Section VII, we introduce a simulation method for the ROS2 scheduler to replicate the timing behavior of ROS2 systems. Additionally, we provide an online end-to-end measurement method that can be applied to existing ROS2 systems and our simulation method to measure the end-to-end timing latencies of the system.
- To compare different system configurations, we evaluate the end-to-end latencies of different systems in a case study in Section VIII. Furthermore, in Section IX, we examine the timing behavior of a basic autonomous driving system that includes a variable number of sensors.

## II. ROS2 SYSTEM MODEL

ROS2 is a set of software libraries for building robot systems and applications. In this section, we explain its architecture, including the main components and interconnects in Section II-A, and the ROS2 scheduler (called ROS2 executor) in Section II-B, as described by previous works [2], [4]. Section II-C explains how to compose a robot system based on the components detailed in Section II-A.

### A. Main Components and Interconnects

We consider a ROS2 system, composed of two types of components, *nodes* and *topics*.

- A *node* represents one component of the system that receives, processes, and forwards data. It consists of timers and subscriptions, as well as the functions that are executed by them. Each timer and subscription is assigned to one specific function of the node, which are called callback functions or *callbacks*.
  - Timers define *time-triggered* callbacks, which access data in the node or receive data from an external interface to process and publish messages to subscriptions or to the underlying robot platform via an external interface.
  - Subscriptions define *event-triggered* callbacks that process received messages. They may store the result in the node or publish the result to subscriptions of other nodes or to the underlying robot platform via an external interface.

We note that a node could also consist of other services, which are irrelevant to our study.

- A *topic* is used as a means of communication among different nodes. It is implemented via data-distribution services (DDS), which provide a publish-subscribe architecture for message transfer. In ROS2, a node can publish a message to a topic, so that all nodes that are subscribed to that topic receive the message.

### B. ROS2 Executor Scheduling

In this paper, we consider the execution of the system on one ECU with one single-threaded *ROS2 executor* that schedules all timer and subscription callbacks of the system nodes.

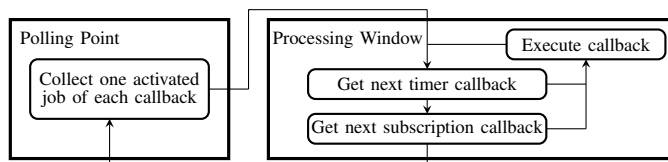


Fig. 1: ROS2 Executor Model

The ROS2 executor implements a custom scheduling policy. It stores all timers and subscriptions of all registered nodes and updates their state during the schedule. Relating this to the classical real-time scheduling theory, a callback function can be seen as a recurrent task and each execution of a callback function is a task instance (or job). A job can reside in one of the following states: *idle*, *activated*, *sampled*, and *running*. There can be several idle jobs of each task being initiated and then being activated by external events. For timers, one job is activated each time its period elapses, while a subscription is activated when it receives a new message. Each timer and subscription has a buffer with a maximum buffer size that stores the currently activated jobs of the task. We note that the jobs of a subscription process the messages in its buffer in a FIFO order. In case the buffer size is not sufficient, under-sampling or message loss may happen. We assume that the buffers are sufficiently large to avoid under-sampling or message loss in all cases.

The scheduling mechanism of the executor is designed to sample and execute jobs with a two-phase design that consists of polling points and processing windows (see Figure 1):

- At each *polling point*, the executor samples the oldest activated job of each task, which will be executed in the next processing window.
- During each processing window, the sampled jobs are executed in the order specified by the executor's scheduling policy. We assume that each timer and each subscription has a unique priority. In ROS2-Foxy (the currently supported version of ROS2), timers have higher priority than subscriptions, and the priorities of timers and subscriptions individually follow the registration order.

After all sampled callbacks are executed, the executor runs the next polling point. If there are no activated jobs at a polling point, the executor spins until an external event takes place, such as a timer period elapsing or message being received.

### C. System Composition

In this subsection, we distinguish several node classes depending on the timers and subscriptions and how they communicate. In addition, we introduce how data is propagated by timers and subscriptions in and between nodes.

A ROS2 system contains nodes that include timers and subscriptions with their corresponding callbacks. Specifically, we consider six node classes, namely *sensor*, *filter*, *subscription actuator*, *timer actuator*, *subscription fusion*, and *timer fusion*. They are classified based on the means of triggering (i.e., timer, callbacks, or a mixture of them) and whether they publish to topics. Table I shows this classification.

TABLE I: Classification of ROS2 Node Classes

	Topic Publication(s)	
	YES	NO
<b>1</b> Timer	<b>Sensor</b>	(not used here)
<b>1</b> Subscription	<b>Filter</b>	<b>Subscription Actuator</b>
<b>&gt;1</b> Subscription	<b>Subscription Fusion</b>	(not used here)
<b>1</b> Timer + <b>≥1</b> Subscription	<b>Timer Fusion</b>	<b>Timer Actuator</b>

These six classes are general enough to compose complex systems. Although we focus on these six classes, our timing analyses can be extended to further classes.

We further classify the communication and the timer and subscription composition of the node classes:

- Three types of communication through callbacks:
  - **O: Inter-node** communication takes place when a callback publishes a message to a topic.
  - **I: Intra-node** communication happens if a callback stores data in the node for other callbacks to access.
  - **E:** For **External** communication, the callback sends (or receives) data to (or from) an external interface.
- The number of timers and subscriptions can be arbitrarily chosen by the user. We assume that nodes can be comprised of the following types of components:
  - **T:** One timer.
  - **S:** One or more subscriptions.

We combine the communication types and node component types. The format represents the components of one node with one or more names that are separated by dashes. Each abbreviation  $XYZ$  includes three parts: the incoming communication type  $X$ , the node component type  $Y$ , and the outgoing communication type  $Z$ . Specifically, we define sensor, filter, and subscription actuator as follows:

- **Sensor (ETO):** A sensor receives data from an external interface, processes it, and publishes a message. It is the first element of the system that generates data.
- **Filter (OSO):** A filter receives messages, processes them, and publishes the result as a message.
- **Subscription Actuator (OSE):** A subscription actuator receives messages, processes them, and sends the result to the robot via an external interface. It is the last element of the system that processes the data.

Timer fusion, subscription fusion, and timer actuator classes include two steps with intra-node communication:

- **Timer Actuator (OSI-ITE):** A timer actuator includes one subscription that receives messages, processes them, and saves the result in the node. The timer accesses the data, processes it, and sends an output signal to the robot at the end of the execution. The timer is the last element of the system that processes the data.
- **Timer Fusion (OSI-ITO):** A timer fusion class features multiple subscriptions that receive messages, process them, and save the result in the node. The timer accesses and combines the data of all callbacks, processes it, and publishes the result as a message.

- **Subscription Fusion (OSI-ISO and OSO):** A subscription fusion class includes multiple subscriptions that receive messages, process them, and either save the result in the node or publish a message. We differentiate between two types of subscriptions, passive and trigger subscriptions. A subscription fusion class includes exactly one trigger subscription. A passive subscription receives a message, processes it, and saves the result in the node. The trigger subscription receives a message, processes it, and triggers the fusion; that is, combining the data of all passive subscriptions and its own data and publishing the result as a message. The fusion is triggered by every execution of the trigger subscription.

Based on these classes, many existing systems can be modeled and analyzed. The analysis does not depend on these specific node classes and instead only analyzes the end-to-end timing behavior of the timers and subscriptions depending on their communication type. As a result, the timing analysis is applicable for any system and the defined node classes only abstract the timers and subscriptions of the node and the intra and inter-node communication for the data propagation between the components in the node and the nodes themselves.

### III. TIMING MODEL

We define the task model in Section III-A. In Section III-B, we introduce the cause-effect chains and job chains in ROS2, for which we specify the end-to-end latencies in Section III-C.

#### A. Task Model

The runtime of the system is managed by an executor that is responsible for dispatching and executing callbacks of a set of nodes that are registered with that executor. Each node can include several timers and several subscriptions. We assume that all nodes are registered to the same executor. This executor is running on a single ECU and schedules all callbacks. In the following we define the tasks of a ROS2 system, which are specified by timers, subscriptions, and their callbacks.

A *timer* is defined by the tuple  $tmr_i = (\tau_i, k_i, pubT_i, sd_i)$ , where the callback task  $\tau_i = (C_i, T_i)$  is specified by its period  $T_i > 0$  and worst-case execution time (WCET)  $C_i \geq 0$ .<sup>1</sup> A timer has a maximum buffer size  $k_i$ , and we assume  $k_i > 1$  for all buffers. We define the current number of elements in the buffer at time  $t$  as  $k_i(t) \leq k_i$ , which is the number of activated jobs of task  $\tau_i$  at time  $t$ . For inter-node communication, the publishing topic  $pubT_i$  specifies to which topic messages are published. It can be *Null*, if the timer does not publish data; for example, if it sends the data to the robot platform instead. For intra-node communication, the subscription dependency  $sd_i$ , which is a subset of the tasks on the same node as  $\tau_i$ , corresponds to the tasks that save data in the node for the callback to access. If  $\tau_j \in sd_i$ , then there is intra-node communication from  $\tau_j$  to  $\tau_i$ . As an example,  $sd_i$  can specify the subscriptions accessed by the timer in a timer fusion class.

<sup>1</sup>We omit the phase, which determines the first activation time, as we always assume the worst case pattern for the upper bound analysis and the online end-to-end measurement method includes the effect of the phase by design.

A *subscription* is defined by the tuple  $sub_i = (\tau_i, k_i, subT_i, pubT_i, sd_i)$ , where the callback task  $\tau_i = (C_i)$  is specified by its WCET  $C_i$ . The current number of messages in the buffer is given by  $k_i(t)$ , which is limited by the maximum buffer size  $k_i$ , with  $k_i > 1$ . The subscription subscribes to the topic  $subT_i$  and may publish to the topic  $pubT_i$  for inter-node communication. We assume that  $\forall i, j : pubT_i \neq pubT_j$ , that is, there can be only one publisher per subscription. If  $pubT_i$  is *Null*, the subscription can either send the data to the robot platform or save it in the node for other callbacks. Please note that  $subT_i$  is required for the triggering and therefore cannot be *Null*. Subscriptions can also include subscription dependencies  $sd_i$ ; for example if they are part of a subscription fusion class.

We denote the finite set of all callbacks included in nodes registered to the executor under analysis as  $\mathbb{T}$ . It includes the set of all timers and subscriptions registered to the executor. We denote the sum of the WCET of all tasks as  $C_{sum} = \sum_{\tau_i \in \mathbb{T}} C_i$ . Each task has its unique priority that is given by the function  $\pi(\cdot)$ . To compare the priorities between callbacks, we use the Iverson Bracket  $[\cdot]$ , which returns 1 or 0 if the condition is true or false, respectively. For example, we determine whether  $\tau_i$  has a higher priority than  $\tau_j$  with  $[\pi(\tau_i) > \pi(\tau_j)]$ . Each task can be scheduled in each processing window and the execution of the task  $\tau_i$  in the  $k$ -th processing window is defined by the job  $j_{i,k}$ . Note that  $j_{i,k}$  does not necessarily exist for all  $k$ , as a callback may not be included in every processing window. We denote a job's start time by  $s_{i,k}$  and the finish time by  $f_{i,k}$ , with  $f_{i,k} \leq s_{i,k} + C_i$  due to the non-preemptive execution of callbacks in ROS2.

The task model in ROS2 is different from standard periodic and sporadic task models. Specifically, tasks do not have a deadline parameter and the total utilization of all executor callbacks is not limited. For example, if the period  $T_i$  is less than the WCET  $C_i$  for a timer, the callback is processed in every processing window and the system is never idle.

### B. Cause-Effect Chains

In this subsection, we introduce cause-effect chains that describe how data propagates through the components of the ROS2 system. The definition of cause-effect chains is inspired by the event-chains of the AUTOSAR Timing Extensions [1], as well as the definition of cause-effect chains by Günzel et al. [10] for periodic and sporadic task systems.

A cause-effect chain  $E = (\tau_1, \dots, \tau_n)$  is a sequence of tasks, with  $n$  tasks in the chain. For the simplicity of presentation, we only focus on one cause-effect chain. For a system with more than one cause-effect chain, each chain should be analyzed and indexed independently. We note that  $C_{sum}$  is the sum of the workload of the whole system independent from the cause-effect chain under analysis. The chains of the system are formed by the communication between the callbacks. In ROS2, inter-node communication takes place if a callback publishes a message to a subscription of another node, while intra-node communication happens if callbacks of the same node access and modify the same data in the node.

The callback  $\tau_i$  sends data via **inter-node communication** to the subscription callback  $\tau_j$  if  $pubT_i = subT_j$ , so that  $\tau_j$  is the successor callback of  $\tau_i$  in the cause-effect chain  $E$ . In this case, each message sent by a job of  $\tau_i$  triggers exactly *one* job of  $\tau_j$ , and this job of  $\tau_j$  processes the message in a future processing window after the message has been published.

The callback  $\tau_j$  accesses data from the subscription callback  $\tau_i$  via **intra-node communication** if  $\tau_i \in sd_j$ , so that  $\tau_j$  is the successor callback of  $\tau_i$  in the cause-effect chain  $E$ . In this case, the same data can be accessed *several times* by different jobs of  $\tau_j$ . Additionally, the callback  $\tau_j$  can access data that is modified by  $\tau_i$  in the same processing window if their jobs are executed in the same processing window and  $[\pi(\tau_j) < \pi(\tau_i)]$ .

For each job  $j_{i,k}$ , we define the read event  $re_{i,k}$  to be at the start time  $s_{i,k}$ , while the write event  $we_{i,k}$  is at the finish time  $f_{i,k}$ . Then for ROS2 cause-effect chains, the following properties define the data propagation for the jobs:

**Definition 1. (Job Chain)** A job chain of  $E$  is a sequence  $jc = (j_{1,\rho(1)}, \dots, j_{n,\rho(n)})$  of data dependent jobs of tasks in  $\mathbb{T}$  with the following properties:

- The entry  $j_{i,\rho(i)}$  is a job of  $\tau_i$  for all  $i \in \{1, \dots, n\}$ .
- For each inter-node dependency ( $pubT_i = subT_{i+1}$ ),  $j_{i+1,\rho(i+1)}$  is the (unique) job that processes the message from  $j_{i,\rho(i)}$ , i.e.,  $we_{i,\rho(i)} \leq re_{i+1,\rho(i+1)}$  holds.
- For each intra-node dependency ( $\tau_i \in sd_{i+1}$ ),  $j_{i+1,\rho(i+1)}$  is a job with  $we_{i,\rho(i)} \leq re_{i+1,\rho(i+1)}$ .

Please note that  $\rho(i) < \rho(i+1)$  for inter-node dependencies, whereas  $\rho(i) \leq \rho(i+1)$  for intra-node dependencies.

Analogous to Günzel et al. [10], we define forward and backward job chains to determine the end-to-end timing behavior of the system. However, since for inter-node communication there is no choice of the jobs in a job chain, only the choice of jobs contributing to intra-node communication are of special interest.

**Definition 2. (Immediate Forward Job Chain)** An immediate forward job chain is a job chain  $jc = (j_{1,\rho(1)}, \dots, j_{n,\rho(n)})$  where  $\forall i \in \{1, \dots, n-1\}$  the following applies: If  $\tau_i \in sd_{i+1}$ , then the job  $j_{i+1,\rho(i+1)}$  is the earliest with  $we_{i,\rho(i)} \leq re_{i+1,\rho(i+1)}$ , i.e.,  $\rho(i+1) = \arg \min_{k \geq \rho(i)} re_{i+1,k} \geq we_{i,\rho(i)}$ .

**Definition 3. (Immediate Backward Job Chain)** An immediate backward job chain is a job chain  $jc = (j_{1,\rho(1)}, \dots, j_{n,\rho(n)})$  where  $\forall i \in \{n, \dots, 2\}$  the following applies: If  $\tau_{i-1} \in sd_i$ , then the job  $j_{i-1,\rho(i-1)}$  is the latest with  $we_{i-1,\rho(i-1)} \leq re_{i,\rho(i)}$ , i.e.,  $\rho(i-1) = \arg \max_{k \leq \rho(i)} we_{i-1,k} \leq re_{i,\rho(i)}$ .

Next, we augment these chains to include external events, so that we can capture the duration between an external event and the sensor sampling, as well as the time between the actuation and the output of the system.

For an immediate forward job chain we denote by  $z$  the time of the external activity and by  $z'$  the time at which the data is processed. We utilize the definition by Günzel et al. [10] to augment the immediate forward job chain and define the job chain whose length corresponds to the reaction time:

**Definition 4.** (*Immediate Forward Augmented Job Chain*) An immediate forward job chain  $jc$  is the unique augmented job chain  $(z, j_{1,\rho(1)}, \dots, j_{n,\rho(n)}, z')$ , such that:

- The external activity  $z$  takes place directly after the sampling of the previous job of  $\tau_1$  before  $j_{1,\rho(1)}$ .
- The sampling happens at the next read-event  $re_{1,\rho(1)}$ .
- The sequence  $(j_{1,\rho(1)}, \dots, j_{n,\rho(n)})$  is an immediate forward job chain.
- The data is processed at time  $z' = we_{n,\rho(n)}$ .

For an immediate backward job chain we denote by  $z$  the time of the sensor sampling and by  $z'$  the time at which an system output is based on the actuation. We augment the immediate backward job chain to determine the chain whose length corresponds to the data age:

**Definition 5.** (*Immediate Backward Augmented Job Chain*) An immediate backward job chain  $jc$  is the unique augmented job chain  $(z, j_{1,\rho(1)}, \dots, j_{n,\rho(n)}, z')$ , such that:

- The output  $z'$  takes place directly before the write event of the next job of  $\tau_k$  after  $j_{n,\rho(n)}$ .
- The actuation happens at the previous write-event  $j_{n,\rho(n)}$ .
- The sequence  $(j_{1,\rho(1)}, \dots, j_{n,\rho(n)})$  is an immediate backward job chain.
- The sampling occurs at time  $z = re_{1,\rho(1)}$ .

### C. End-To-End Latencies

In this subsection, we define the end-to-end latencies that are analyzed in this paper, namely maximum reaction time and maximum data age for a specific cause-effect chain, based on the job chains introduced in Section III-B.

In ROS2, each cause-effect chain (or, in short, chain) starts with a sensor node and ends with an actuator node. Hence, the first task of the chain is a timer callback, while all other tasks are either timer or subscription callbacks. Job chains represent specific instances of a cause-effect chain; that is, the timing of processing one specific external signal.

The maximum reaction time is the maximum latency for an external signal to be processed by the actuator. For example, it is the largest interval between a user pressing a button to lock the car's doors and them actually being locked. The maximum data age corresponds to the maximum duration between a sensor sampling and an output being based on that sample. For example, it is the maximum length between the current camera image sampling and the latest time at which the steering controls are based on that camera sample. The maximum reaction time and maximum data age of a cause-effect chain correspond to the supremum over all immediate forward and backward augmented job chains, respectively.

An example system is shown in Figure 2. It includes two sensor nodes, which publish data to the corresponding sensor topics. The fusion node features one subscription per sensor and a timer that publishes data to the fusion topic. The actuator includes one subscription that subscribes to the fusion topic. The system includes two cause-effect chains, each of which consists of one sensor timer, one fusion subscription, one fusion timer, and one actuator subscription.

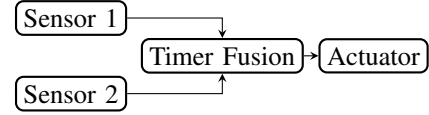


Fig. 2: A fusion system that includes two sensors, one timer fusion and one actuator node. The timer fusion consists of one subscription per sensor and one timer to publish the fusion results. The system includes two cause-effects chains.

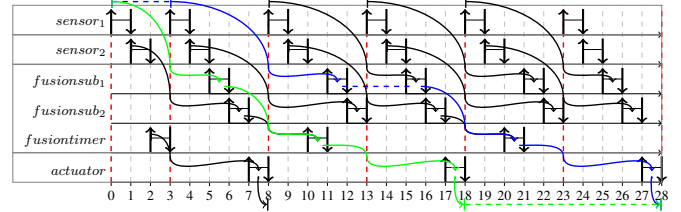


Fig. 3: Example schedule for the system shown in Fig. 2. Each box represents one node and its callbacks. The schedule includes polling points (red dashed lines) and processing windows. The arrows represent the data propagation between jobs. The reaction time (blue) and data age (green) are shown for the chain start starts from the first sensor, and includes the fusion subscription and timer, and the actuator subscription.

Figure 3 shows an example schedule for the fusion system in Figure 2. Each box specifies one node and the callbacks that are part of it. The schedule includes the polling points, which are indicated by the red dashed vertical lines, while each processing window is given by the interval between two successive polling points. In addition, the release time and finish time of each job is indicated by the upwards and downwards pointing arrows, respectively. In this schedule, the sensor timers are executed in every processing window, while the fusion timer is executed in every second processing window. For ease of presentation, all callbacks execute as long as their worst-case execution time  $C_i = 1$  in this schedule.

The data propagation between the callbacks is shown by the black, green, and blue arrows. The inter-node communication takes place between the sensor and fusion subscriptions, as well as the fusion timer and actuator subscription, while the intra-node communication takes place between the fusion subscriptions and fusion timer. In this schedule, callbacks always process messages from previous processing windows.

The blue and green paths represent the immediate forward and backward augmented job chains for the reaction time and data age, respectively. As introduced in Section III-B, the blue path is an immediate forward augmented job chain  $(z, j_{1,\rho(1)}, \dots, j_{n,\rho(n)}, z')$ . The external event  $z$  happens right after time 0 and is sampled at time 3. The reaction time is the difference between the external event and the actuator processing it at time 28, i.e., it is  $28 - 0 = 28$  in this case. Likewise, the data age corresponds to the green path, which is an immediate backward augmented job chain  $(z, j_{1,\rho(1)}, \dots, j_{n,\rho(n)}, z')$ . For this chain, the data is sampled at time 0 and processes new data at time 28, i.e., the data age is  $28 - 0 = 28$ .

#### IV. RELATED WORK

The Robot Operating System (ROS) [15], which is a set of software libraries for building robot applications, was released in 2007. It provides functionalities to implement basic components as nodes that communicate via topics. Additionally, there are many available packages that provide basic components of robot systems for a variety of applications, such as warehouse robots and autonomous driving. However, ROS does not natively support real-time programming. Although some extensions, such as RT-ROS [20] and ROSCH [16] extend the ROS architecture to support some real-time features, they are not widely adopted as they are not part of the core architecture.

In 2017, the first version of ROS2 was released, which built upon the core concepts of ROS, such as nodes and topics, but improved upon many aspects, such as the support for real-time code and the use of DDS [14] for secure and real-time inter-node communication. In addition, it includes a new scheduler designs for the executor that manages the execution of the time-triggered and event-triggered function of the system.

In the following years, the ROS2 executor was analyzed, including response time analysis when modeling the ROS2 components as a DAG [2], [4], or as processing chains [18]. For such systems, each component directly triggers the components they are connected to. In addition, optimization for the priority assignment of tasks was proposed by Choi et al. [5]. However, these results do not explicitly consider the data propagation between the sampling and the actuation when modeling the tasks as cause-effect chains.

End-to-end timing analysis of cause-effect chains for real-time systems have been studied over decades. In 2009, Feiertag et. al. [8] proposed the first end-to-end latency semantics to define the maximum reaction time and maximum data age. The subsequent work can be classified into two categories. So-called active approaches control the release of jobs in the chain to ensure the correctness of data reading and writing, e.g., [9], [17]. The upper bound analysis in this work is a passive approach that analyzes the end-to-end latency based on a given set of tasks and dependencies. For sporadic and periodic task systems, multiple end-to-end analysis can be found in the literature [6], [7], [10], [12]. Since these approaches are designed for periodic or sporadic task systems, they are not directly applicable to ROS2 systems, which feature a combination of time-triggered and event-triggered functions. Thus, our work is the the first to consider end-to-end timing analysis for cause-effect chains in ROS2.

#### V. DELIMITATION AND DISCUSSION OF RELATED WORK

In this section, we emphasize and discuss the differences between our work and previous research results in the domain of end-to-end latency analyses for ROS2 systems. A summary is provided in Table II, that includes the execution model, timing metric, analyzed chain structure, communication types, number of executors, and the OS overhead. Note that SBF refers to supply bound function for the OS overhead. Additionally, we use regular expressions for the chain structure that include timers and subscriptions as  $T$  and  $S$ , respectively.

**Casini et al. [4] and Blass et al. [2]** both provide a worst-case response time analysis for processing chains, considering multiple executors and operating system overheads using supply-bound functions. They analyze processing chains consisting of one triggering timer at the start and multiple chained callbacks. Each callback is directly triggered by the finishing of the preceding callback, and each callback is allowed to have multiple predecessors and successors. Notably, their proposed model of computation implies that the callbacks only communicate via the publish-subscribe architecture of DDS, which corresponds to the inter-node communication in our work. The analyzed timing metric is the *maximum response time*, which is the maximum time between release of the timer at the beginning of the chain and the completion of all chain callbacks.

In contrast, the focus of our work is the temporal behavior of data propagation through the system, considering different end-to-end semantics. In particular, we guarantee that each callback execution processes the data of all chains that it is part of. In [2], [4] the maximum response time specified is the maximum time until a callback is executed. However, a subscription job only processes the oldest message in the buffer, so that a processed message may not originate from the analyzed chain if the buffer includes multiple messages from different publishers. As a result, messages may be processed in a later processing window or may be lost due to buffer overflow. To circumvent this, we limit the number of predecessors to one per subscription. We consider a single executor and do not consider any operating system overheads, as we focus on the data propagation between callbacks, including inter- and intra-node communication. On the upside, our work is more general with respect to the admissible chain structures. That is, only the first callback is limited to a timer and each subsequent callback can be either a timer or a subscription, while we do not allow consecutive timers in a cause-effect chain. This allows us to consider chains that include multiple individually triggered timers and chains with callbacks that propagate data without triggering the successor callback directly. Furthermore, the metrics are different, as our analysis does not only specify the worst-case response time, which corresponds to the maximum difference between the start time of the first chain callback and the finish time of the last chain callback. In contrast, we consider the MRT and MDA, which include the additional time from the external activity until the data sampling and the time between an actuation and the output. In comparison, the maximum response time corresponds to the maximum *reduced* reaction time as defined in [10].

In consequence of the different focuses, systems that can be analyzed by both [2], [4] and our work would consider: (1) a single executor without operating system overheads, and (2) a single chain that only includes a timer and multiple subscriptions with inter-node communication. In such a system, neither the strengths and focus of our work (i.e., different message transmission, system structure, and end-to-end semantics) nor of [2], [4] (i.e., the supply-bound function and the multiple executors) are considered. Therefore, a direct comparison would focus on a degenerate case of both analyses.

TABLE II: Related Works Contribution Overview

Related Work	Exec. Model	Timing Metric	Chain Structure	Communication	No. Executors	Overhead
Casini et al. [4]	ROS2	Max. Response Time	TS*	Inter-Node	Multiple	SBF
Blass et al. [2]	ROS2	Max. Response Time	TS*	Inter-Node	Multiple	SBF
Tang et al. [18]	ROS2	Max. Response Time	TS*	Inter-Node	Single	SBF
Several [6], [7], [10], [12]	Periodic	MRT & MDA	T*	Inter-Task	–	–
Our	ROS2	MRT & MDA	T(S ST)*	Inter-/Intra-Node	Single	–

**Tang et al. [18]** analyze the worst-case response time of processing chains for a model similar to the once considered by Casini et al. [4] and Blass et al. [2]. The main difference is that they consider the impact of the priority assignment for callbacks to analyze the worst-case response time. As a result, a comparison would result in the same simplification and problems as for Casini et al. [4] and Blass et al. [2].

**Davare et al. [6], Dürr et al. [7], Günzel et al. [10] and Kloda et al. [12]** provide a *maximum reaction time* and/or *maximum data age* analysis of cause-effect chains consisting of periodic tasks in a uniprocessor system. Their system model is incompatible with our work. In particular, only a set of periodic tasks that is scheduled in a preemptive fixed-priority manner is considered. Event-triggered execution, which is an essential component of the ROS2 architecture, is not considered in their model. Moreover, Günzel et al. [10] requires fixing the execution time to the worst case, and the worst-case response-time analysis, that is required for the maximum reaction time and maximum data age analysis in [6], [7], [12], is not applicable to the ROS2 executor/scheduler.

## VI. CAUSE-EFFECT CHAIN UPPER BOUND ANALYSIS

In this section, we present how to calculate an upper bound on the maximum reaction time and maximum data age given a chain  $E = (\tau_1, \dots, \tau_n)$ . The system consists of the node classes, timers, and subscriptions that are introduced in Section II-C. We assume a DDS with synchronous message passing, where the execution time includes the time for publishing a message. As a result, all messages are guaranteed to be transferred when a callback finishes. Since we assume that there is only one publisher per subscription, there is at most one message published to each topic per processing window. This message is directly processed (and removed) in the *subsequent* processing window. Please note that because of  $k_i > 1$  no buffer overflow can occur.

We first provide an upper bound on the maximum reaction time in Theorem 1 and that on the maximum data age in Corollary 1. Specifically, Table III presents the callbacks that are added to the corresponding cause-effect chain by the node types and which upper bound type they contribute to the total upper bound of the cause-effect chain.

**Theorem 1.** *Under the assumption of a DDS with synchronous message passing,  $\tau_1$  is a sensor timer task and  $\tau_n$  is an actuation task, the maximum reaction time of a cause effect chain  $E = (\tau_1, \dots, \tau_n)$ , is at most  $\sum_{i=1}^n ub(\tau_i)$ , where*

TABLE III: Classification of ROS2 Callback Classes

Node class	Chain Callbacks	Upper Bound Types
Sensor	$tmr_i$	$ub_{st}(\tau_i)$
Filter	$sub_i$	$ub_{as}(\tau_i)$
Subscription Actuator	$sub_i$	$ub_{as}(\tau_i)$
Timer Fusion	$sub_i + tmr_j$	$ub_{ps}(\tau_i) + ub_{tt}(\tau_j)$
Subscription Fusion	$sub_k$ or $sub_i + sub_j$	$ub_{ts}(\tau_k)$ or $ub_{ps}(\tau_i) + ub_{ts}(\tau_j)$
Timer Actuator	$sub_i + tmr_j$	$ub_{ps}(\tau_i) + ub_{tt}(\tau_j)$

$$ub(\tau_i) = \begin{cases} ub_{st}(\tau_i) & \text{if } \tau_i \text{ a sensor timer} \\ ub_{tt}(\tau_i) & \text{if } \tau_i \text{ an trigger timer} \\ ub_{as}(\tau_i) & \text{if } \tau_i \text{ an active subscription} \\ ub_{ps}(\tau_i) & \text{if } \tau_i \text{ a passive subscription} \\ ub_{ts}(\tau_i) & \text{if } \tau_i \text{ a trigger subscription} \end{cases}, \quad (1)$$

and  $ub_{st}(\tau_i)$ ,  $ub_{tt}(\tau_i)$ ,  $ub_{as}(\tau_i)$ ,  $ub_{ps}(\tau_i)$ , and  $ub_{ts}(\tau_i)$  are defined in Eqs. (4), (5), (6), (7), and (8), respectively.

*Proof.* As defined in Section III-B, let  $j_{i,\rho(i)}$  be the job of task  $\tau_i$  that is executed in the  $\rho(i)$ -th processing window. Recall that  $re_{i,\rho(i)}$  is the moment of its read event and also its start time, whereas  $re_{i,\rho(i)} + C_i$  is the upper bound on the moment of its write event. We know that  $re_{i,\rho(i)} + C_i$  is *no more* than the finishing time of the  $\rho(i)$ -th processing window of the executor. There are two cases due to the non-preemptive schedule of the ROS2 executor:

- If the data of  $j_{i,\rho(i)}$  is sent to the next task  $\tau_{i+1}$  via inter-node communication, then the next job in the immediate forward augmented job chain is processed in the  $(\rho(i) + 1)$ -th processing window. That is,  $\rho(i + 1)$  is  $\rho(i) + 1$ .
- If the data of  $j_{i,\rho(i)}$  is sent to the next task  $\tau_{i+1}$  via intra-node communication, then the next job in the immediate forward augmented job chain is processed in the  $\rho(i + 1)$ -th processing window, with  $\rho(i + 1) \geq \rho(i)$ .

Suppose  $\theta_i$  is the finishing time the  $\rho(i)$ -th processing window for job  $j_{i,\rho(i)}$ . By definition, the length of an immediate forward augmented job chain  $jc$  is

$$z' - z = \theta_1 - z + \left( \sum_{i=2}^n \theta_i - \theta_{i-1} \right) + z' - \theta_n \quad (2)$$

In the followings, we provide bounds on each of these terms:

**Bound on  $z' - \theta_n$ :** Since  $\tau_n$  is an actuator by assumption, we know that  $z'$  is equal to  $w_{e_{n,\rho(n)}} \leq \theta_n$ . Therefore,  $z' - \theta_n \leq 0$ .

**Bound on  $\theta_1 - z$ :** Due to the assumption that there is always a timer at the beginning,  $E$  starts with a sensor timer task  $\tau_1$ .



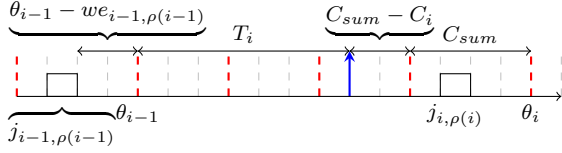


Fig. 4: Example schedule for Lemma 1. The blue arrow marks release of job  $j_{i,\rho(i)}$ , dotted red lines represent polling points.

For the upper bound of  $\theta_1 - z$ , the external event  $z$  happens right after the last sensor timer job  $j_{1,k}$  before  $j_{1,\rho(1)}$  finishes. After that, the timer callback is sampled after its period  $T_1$  elapses. In the worst case, its period elapses right after a processing window starts that includes every callback except  $\tau_1$ , resulting in an additional delay of  $C_{sum} - C_1$ . Afterwards, the timer is executed together with every callback, resulting in a delay of  $C_{sum}$ . As a result,  $\theta_1 - z$  is upper bounded by:

$$\theta_1 - z \leq T_1 - C_1 + 2 \cdot C_{sum} \quad (3)$$

We denote this as the **Sensor Timer** upper bound for task  $\tau_i$ :

$$ub_{st}(\tau_i) = T_i - C_i + 2 \cdot C_{sum} \quad (4)$$

**Bound on  $\theta_i - \theta_{i-1}$ :** To improve readability, we show in Lemmas 1 to 4, that  $\theta_i - \theta_{i-1}$  is upper bounded by  $ub_{tt}(\tau_i)$ ,  $ub_{as}(\tau_i)$ ,  $ub_{ps}(\tau_i)$ , and  $ub_{ts}(\tau_i)$  when  $\tau_i$  is a trigger timer, an active subscription, a passive subscription, and a trigger subscription, respectively. Combining these results with the argumentation so far proves the theorem.  $\square$

**Lemma 1 (Trigger Timer).** *If  $\tau_i$  is a trigger timer task, then  $\theta_i - \theta_{i-1}$  in Eq. (2) is at most*

$$ub_{tt}(\tau_i) = T_i - C_i + 2 \cdot C_{sum} \quad (5)$$

*Proof.* Due to the ROS2 executor design, timers are executed before subscriptions in a processing window. As specified in Table III, the job  $j_{i-1,\rho(i-1)}$  is a subscription job. Therefore, the trigger timer job  $j_{i,\rho(i)}$  can not be executed before  $\theta_{i-1}$ . Additionally, the job  $j_{i-1,\rho(i-1)}$  is guaranteed to finish before  $\theta_{i-1}$ , so that  $we_{i-1,\rho(i-1)} \leq \theta_{i-1}$ . At the earliest, the job  $j_{i,\rho(i)}$  is sampled at  $\theta_{i-1}$ , so that it is guaranteed to finish no later than  $\theta_{i-1} + C_{sum}$ . At the latest, as illustrated in Figure 4, the timer elapses after  $\theta_{i-1} + T_i$  right after a processing window starts that includes every callback except  $\tau_i$ , resulting in an additional delay of  $C_{sum} - C_i$ . Therefore, the job  $j_{i,\rho(i)}$  is sampled no later than  $\theta_{i-1} + T_i + C_{sum} - C_i$ . The processing window  $\rho(i)$  of job  $j_{i,\rho(i)}$  has a maximum length of  $C_{sum}$ . As a result,  $\theta_i - \theta_{i-1} \leq T_i - C_i + 2 \cdot C_{sum}$ .  $\square$

Active subscriptions receive messages, process them, and send the result to the robot platform or publish a message. This case only covers the subscription of the **subscription actuator** class and **filter** classes, but not fusion or timer actuator classes.

**Lemma 2 (Active Subscription).** *If  $\tau_i$  is an active subscription task, then  $\theta_i - \theta_{i-1}$  in Eq. (2) is at most*

$$ub_{as}(\tau_i) = C_{sum} \quad (6)$$

*Proof.* Since the subscription always processes a message in the following processing window in the ROS2 system model,  $\rho(i)$  is equal to  $\rho(i-1) + 1$  in this case. Therefore, by definition, each processing window takes at most  $C_{sum}$  of time and  $\theta_i - \theta_{i-1} \leq C_{sum}$  for this case.  $\square$

For **timer fusion**, **subscription fusion**, and **timer actuators**, such passive subscriptions only receive, process, and save the result in the node, so that it can be accessed by the timers and the trigger subscription of these classes.

**Lemma 3 (Passive Subscription).** *If  $\tau_i$  is a passive subscription task, then  $\theta_i - \theta_{i-1}$  in Eq. (2) is at most*

$$ub_{ps}(\tau_i) = C_{sum} \quad (7)$$

*Proof.* The proof is identical to the proof of Lemma 2.  $\square$

Trigger subscriptions combine the data of all subscriptions in the node and send the result as a message. A subscription fusion node consists of multiple subscriptions, including one trigger subscription. The fusion is triggered every time the trigger subscription is executed, which happens every time it processes a received message of its predecessor task, which may be part of the chain  $E$  or a different chain in the system.

**Lemma 4 (Trigger Subscription).** *If  $\tau_i$  is a trigger subscription task, then  $\theta_i - \theta_{i-1}$  in Eq. (2) is at most*

$$ub_{ts}(\tau_i) = \begin{cases} C_{sum} & \text{if } \tau_{i-1} \notin sd_i \\ \sum_{\bar{\tau}_k \in \bar{E}} ub(\bar{\tau}_k) + C_{sum} & \text{if } \tau_{i-1} \in sd_i \end{cases} \quad (8)$$

where the chain  $\bar{E} = (\bar{\tau}_1, \dots, \bar{\tau}_m)$ <sup>23</sup> triggers task  $\tau_i$  i.e., task  $\bar{\tau}_1$  is a timer,  $(\bar{\tau}_2, \dots, \bar{\tau}_m)$  are subscriptions, and  $pubT_m = subT_i$ .

*Proof.* We consider two cases, depending on whether the task  $\tau_{i-1}$  is in  $sd_i$ : the task  $\tau_i$  accesses data of  $\tau_{i-1}$  via intra-node communication if  $\tau_{i-1} \in sd_i$ , or  $\tau_i$  receives data via inter-node communication if  $\tau_{i-1} \notin sd_i$ .

**Case 1: Inter-node:** If  $\tau_{i-1} \notin sd_i$ ,  $\tau_{i-1}$  and  $\tau_i$  communicate via inter-node communication and the subscription is processed in the next processing window, i.e.,  $\rho(i)$  is equal to  $\rho(i-1) + 1$ , leading to  $\theta_i - \theta_{i-1} \leq C_{sum}$ .

**Case 2: Intra-node:** If  $\tau_{i-1} \in sd_i$ , then there is intra-node communication between  $\tau_{i-1}$  and  $\tau_i$ , and  $j_{i,\rho(i)}$  is not directly triggered by  $j_{i-1,\rho(i-1)}$  but by a job of  $\bar{\tau}_m$ .

To find such a job that triggers  $j_{i,\rho(i)}$  (if it was not triggered before), let  $t \in \mathbb{N}$  such that  $\bar{j}_{1,t}$  is the first job of  $\bar{\tau}_1$  executed after  $\theta_{i-1}$ . Then the following holds:

- $\bar{re}_{1,t-1} \leq \theta_{i-1}$
- The immediate forward chain starting at  $\bar{j}_{1,t}$  ends at a job  $\bar{j}_{m,q}$  of  $\bar{\tau}_m$ , with  $q \in \mathbb{N}$ , that triggers  $j_{i,\rho(i)}$  (if it was not triggered before).

Hence,  $j_{i,\rho(i)}$  is executed in the  $(q+1)$ -th processing window.

<sup>2</sup>Please note that the indices of this chain  $\bar{E}$  are unrelated to the chain  $E$  under analysis and that they do not share callbacks.

<sup>3</sup>Each callback in  $\bar{E}$  is triggered by inter-node communication. Starting from  $\tau_i$ ,  $\bar{E}$  can be constructed by adding the preceding publisher callback to the head of the chain until a timer has been added.

The maximum reaction time of the chain  $\bar{E}$  covers the time from  $\theta_{i-1}$  until  $\overline{we_{m,q}}$ . The upper bound  $\sum_{\bar{\tau}_k \in \bar{E}} ub(\bar{\tau}_k)$  covers also the time from  $\theta_{i-1}$  until the *end of the processing window* of job  $\bar{j}_{m,q}$ . Moreover, the length of the  $(q+1)$ -th processing window is upper bounded by  $C_{sum}$ . Therefore,  $\theta_i - \theta_{i-1} \leq \sum_{\bar{\tau}_k \in \bar{E}} ub(\bar{\tau}_k) + C_{sum}$ .  $\square$

**Corollary 1.** *Under the same assumption of Theorem 1, the maximum data age is upper bounded by  $\sum_{i=1}^n ub(\tau_i)$ , where  $ub(\tau_i)$  is defined in Eq. (1).*

*Proof.* Let  $\tau_k$  be the last timer task in the cause-effect chain. By definition, such a task  $\tau_k$  exists, as the first task  $\tau_1$  is a sensor timer task. Therefore,  $1 \leq k \leq n$ . By the definition of an immediate backward augmented job chain,  $z'$  happens directly before the next write event of the next job of  $\tau_n$  after  $\bar{j}_{n,\rho(n)}$ . By definition, the length of an immediate backward augmented job chain  $j_c$  is

$$z' - z = \psi_1 - z + \left( \sum_{i=2}^k \psi_i - \psi_{i-1} \right) + (z' - \psi_k)$$

with  $\psi_i$  being the beginning of the  $\rho(i)$ -th processing window. A similar proof as for Theorem 1 can be done to show that  $\psi_1 - z + \left( \sum_{i=2}^k \psi_i - \psi_{i-1} \right) \leq \sum_{i=1}^{k-1} ub(\tau_i)$ .

Here, we only sketch the proof of  $z' - \psi_k$ . Since  $\tau_k$  is the latest timer of the cause-effect chain, the time between the write event  $we_{k,\rho(k)}$  and the next write event of  $\tau_k$  is upper bounded by  $T_k - C_k + 2 \cdot C_{sum}$ . Furthermore,  $\tau_{k+1}, \tau_{k+2}, \dots, \tau_n$  are only subscription tasks. Therefore, the jobs of  $\tau_{k+1}, \tau_{k+2}, \dots, \tau_n$  in a backward augmented job chain are executed in consecutive processing windows. Hence,  $z' - \psi_k \leq (n-k)C_{sum} + T_k - C_k + 2 \cdot C_{sum} = ub_{tt}(\tau_k) + \sum_{i=k+1}^n ub(\tau_i)$ , where  $ub(\tau_i)$  is either  $ub_{as}(\tau_i)$  or  $ub_{ts}(\tau_i)$  for  $i = k+1, k+2, \dots, n$ . Thus, we reach the conclusion.  $\square$

## VII. ONLINE END-TO-END ANALYSIS

The upper bound analysis in Section VI is pessimistic compared to the real end-to-end latencies of the system, as it assumes the worst-case execution pattern in all cases. In Section VII-A, we introduce a method to simulate ROS2 systems with a single executor to determine a lower bound on the timing values.<sup>4</sup> Additionally, we introduce an online end-to-end timing measurement method in Section VII-B to determine the maximum reaction time and the maximum data age of all cause-effect chains. This method can be applied to existing ROS2 systems and our simulation approach to compare our lower bound and the real observed values.

### A. Executor Simulation

This subsection introduces how to simulate the executor and callback execution of a ROS2 system on a single ECU.

<sup>4</sup>We only consider the execution scenario by fixing the execution time of each task to its worst-case execution time. For this scenario we observe the exact maximum reaction time and maximum data age. However, since this does not cover all possible execution scenarios, the measured values are just lower bounds for the general case.

---

### Algorithm 1 Executor Simulation

---

```

1: procedure SIMULATEEXECUTORPROCESSINGWINDOW
2:   updateTimerBuffers()
3:   readyTimers = getReadyTimers()
4:   readySubscriptions = getReadySubscriptions()
5:   pastPollingPoints.append(now)
6:   executeTimers(readyTimers)
7:   executeSubscriptions(readySubscriptions)
8:   if length(getReadyCallbacks()) == 0 then
9:     skipToNextPollingPoint()

```

---

For the simulation, we define a system state that consists of the global time, the past polling points, and the nodes that consist of multiple callbacks. During the simulation, we simulate the execution of callbacks by elapsing the global time by the execution time of each callback, and updating the buffer states of all timer and subscription callbacks.

The simulation of the system is detailed in Algorithm 1. We simulate the schedule considering the global time and past polling point times. Line 2 updates the activation buffer  $k_i(t)$  for each timer. The function determines the difference in activations between the previous and current polling point and adds it to the timer buffer. Lines 3-4 collect all callbacks with a non-empty buffer, after which Line 5 adds the current time to the past polling points. Lines 6-7 execute all timer and subscription callbacks, given their priority order. For each callback, the global time is advanced by its execution time. Lines 8-9 skip to the next polling point and advance the global time to the next callback activation if no job is activated.

### B. Online Timing Measurement

In this subsection, we introduce an online end-to-end timing measurement method to determine the end-to-end timing latencies of existing ROS2 systems and of the simulation approach that is presented in the previous subsection. For the timing measurement, we introduce a new message header, which is a message itself, that can be added to existing message types in ROS2 and stores the timing information to calculate the reaction time and data age of all job chains. A message contains a list of entries, each of which represents one job chain. Each entry contains a unique identifier, the reaction time origin date, and the data age origin date. The unique identifier is a list of callbacks that processed the message so far. Each callback adds its unique identifier, such as a name, to the history during its execution. The origin dates for the reaction time and data age are required to determine the maximum reaction time and maximum data age and are set once by the sensor timers during their execution. For each sensor timer execution  $j_{i,k}$ , the data age origin date corresponds to the start time  $s_{i,k}$ . The reaction time origin date is the start time of the previous execution  $s_{i,k-1}$ , as shown in Figure 3.

With this approach, each callback determines the end-to-end latencies of all chains that end with the callback itself. As a result, the maximum reaction time and maximum data age of all sub-chains of the system are measured during execution. Furthermore, the end-to-end latencies of the complete chains are stored in the actuator callbacks of the system.

---

**Algorithm 2** Message Creation

---

```
1: procedure CREATEMESSAGE
2:   if type == Timer then
3:     msg = Message()
4:   else
5:     msg = DDSBuffer.pop()
6:   for forwardMessage ∈ forwardBuffer do
7:     for entry ∈ forwardMessage do
8:       msg.addEntry(entry)
9:   forwardBuffer.clear()
10:  return msg
```

---

---

**Algorithm 3** Subscription Execution

---

```
1: procedure EXECUTESUBSCRIPTION
2:   now += wcet
3:   updateAnalysisDataAge()
4:   msg = createMessage()
5:   updateLatestMessage(msg)
6:   updateMessageRegisters()
7:   updateAnalysisRegisters()
8:   forwardMessage(msg)
9:   sendMessage(msg)
```

---

For each callback, we add two register types, namely the message and analysis registers for each timing value, resulting in four different registers, as well as a forward buffer that stores messages of subscription dependencies for subscription fusion, timer fusion, and timer actuator classes.

The message registers store the entries of processed messages. Each time a callback is executed and processes a message, it updates the origin dates of existing entries with the message entries. The analysis register saves the maximum reaction time and maximum data age of all entries, which is the maximum difference between the current execution time and the origin dates of the processed entries. During each callback execution, the analysis register values are updated with the entries that are stored in the message register, including new entries that are stored in the processed message. The forward buffer is used for intra-node communication and stores messages that are forwarded by subscription dependencies. In general, reaction time is updated before a send operation, while data age is updated before receive and send operations.

Algorithm 2 details the message creation for all callbacks. For timers, Lines 2-3 create a new empty message, while subscriptions take the newest message in the buffer in Lines 4-5. For fusion nodes and timer actuators, Lines 6-9 collect all entries from forwarded messages of subscription dependencies, after which the forward buffer is cleared.

The next part is the subscription execution, which is detailed in Algorithm 3. First, Line 2 executes the function of the subscription. We assume each callback executes according to its WCET. Line 3 updates the maximum data age of the analysis registers with the entries that are saved from the previous executions. Lines 4-5 create and update the latest message. After that, Line 6 updates the message registers with the entries of the new message. Then, Line 7 updates the analysis registers for both the maximum reaction time and maximum data age with the new message register contents.

---

**Algorithm 4** Timer Execution

---

```
1: procedure EXECUTETIMER
2:   activationBuffer--
3:   msg = createMessage()
4:   if sdi == None then
5:     if hasLatestMessage() then
6:       msg.addEntry(last, now, [id])
7:     else
8:       msg.addEntry(now, now, [id])
9:   now = now+wcet
10:  updateAnalysisDataAge(now)
11:  updateLatestMessage(msg)
12:  updateMessageRegisters()
13:  updateAnalysisRegisters(now)
14:  sendMessage(msg)
```

---

Line 8 forwards the message to all callbacks that include the subscription as a subscription dependency. Additionally, it adds the forward callback to the history of all entries of the forwarded message. Finally, Line 9 sends a message so that the subscription with  $sub_j$  with  $subT_j = pubT_i$  receives it.

Next is the execution of timers, which are part of sensors, timer fusion, and timer actuators. Timers cannot directly process received messages, but instead create new messages from sensor data or process data from subscription dependencies.

Algorithm 4 details the timer execution and the updating process for the timing values. Line 2 decreases the activation buffer, as the timer is executed. Lines 3-8 create the message. For fusion and actuator timers, Line 3 collects the messages from all subscription dependencies that are stored in the forward buffer. For sensor timers, Lines 4-8 create the first entry of the message. For the first timer execution, the current time  $now$  is used for both reaction time and data age origin dates. For all other executions, the data age origin date is the current time  $now$ , while the reaction time origin date is the start time of the previous execution  $last$ . Line 9 represents the callback execution. We assume each callback executes as long as its WCET. After that, the timing analysis values are updated for the analysis and message registers.

The data age analysis register is updated with the previous message register entries in Line 10. Then, the latest message is updated in Line 11. The new message is used in Line 12 to update the entries in the message registers. After that, Line 13 updates the analysis registers, including the maximum reaction time and maximum data age using the new values in the message register. Finally, Line 14 publishes the message, so that subscriptions  $sub_j$  with  $subT_j = pubT_i$  receive it.

With this method, existing ROS2 systems can measure the end-to-end timing values of all chains. After the execution, each callback includes an entry for each chain in its analysis register that ends with the callback itself. The maximum reaction time and maximum data age of each complete cause-effect chain is stored in the analysis registers of each actuator callback. In addition, each entry includes a list of the callbacks that are part of the chain. This method can be applied to the executor simulation in Subsection VII-A and to existing ROS2 systems to measure the end-to-end timing latencies.

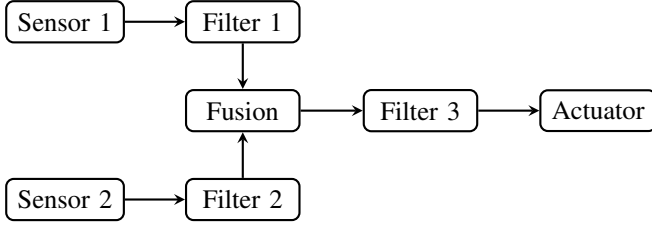


Fig. 5: Fusion system with two chains as case-study.

TABLE IV: Analysis for over-utilized system

System	Chain	$C_{chain}$ [ms]	Upper bound [ms]	Lower Bound [ms]	Observed [ms]
subscription fusion + subscription actuation	Chain1	110.0	1160.0	1080.0	1090.0
	Chain2	160.0	1950.0	1070.0	1080.0
subscription fusion + timer actuation	Chain1	140.0	1797.5	1320.0	1330.0
	Chain2	190.0	2722.5	1310.0	1320.0
timer fusion + subscription actuation	Chain1	140.0	1797.5	1470.0	1480.0
	Chain2	160.0	1787.5	1460.0	1470.0
timer fusion + timer actuation	Chain1	170.0	2570.0	1770.0	1780.0
	Chain2	190.0	2560.0	1760.0	1770.0

### VIII. CASE STUDY

We examine the end-to-end latencies of the system in Figure 5. Specifically, we calculate the upper bounds based on the analysis in Section VI, and apply the simulation according to Section VII-A as well as the online measurement method from Section VII-B to the real system in ROS2.

The system in Figure 5 consists of two sensors, three filters, one fusion class, and one actuator class. The sensors and filters are implemented with the sensor timer and filter classes from Section II-C. For the fusion and actuator node, we compare the timing behavior between the subscription-based and timer-based types of each class. As a result, we evaluate four different system types. For each class, the number of callbacks per chain changes, which we specify for each chain in the analysis. For example, a subscription actuator only includes one callback, while a timer actuator includes two for each chain that it is part of. We further configure the subscription fusion class to utilize the subscription of *filter1* as the trigger subscription, while *filter2* is a passive subscription.

For each component, we set the execution time of the callbacks and the period of the timers. We consider two different cases, specifically an *over-utilized system* and an *under-utilized system*. Let  $C_{sum}$  be the sum of all callback execution times. For an over-utilized system,  $C_{sum} > T_i$  for all timers  $tmr_i$ , while  $C_{sum} < T_i$  for an under-utilized system. For an over-utilized system, the periods of the timers are set to  $T_i = \frac{C_{sum}}{4}$  for sensor class nodes and to  $T_i = \frac{C_{sum}}{2}$  for the timer fusion and timer actuator. For an under-utilized system, we set the period to  $T_i = C_{sum} \cdot 2$  for the sensors and  $T_i = C_{sum} \cdot 4$  for timer fusion and timer actuators. For each sensor and filter, we set the execution time such that  $C_{sensor1} = C_{filter1} = 10$  ms,  $C_{sensor2} = C_{filter2} = 20$  ms, and  $C_{filter3} = 30$  ms. For the fusion block, we set the execution time of all timer and subscription callbacks  $\tau_i$  to  $C_i = 30$  ms. We assume each callback executes as long as its WCET and all callbacks have a buffer size of  $k_i > 1$ .

TABLE V: Analysis for under-utilized system

System	Chain	$C_{chain}$ [ms]	Upper bound [ms]	Lower Bound [ms]	Observed [ms]
subscription fusion + subscription actuation	Chain1	110.0	1430.0	540.0	550.0
	Chain2	160.0	2490.0	530.0	540.0
subscription fusion + timer actuation	Chain1	140.0	2900.0	1320.0	1330.0
	Chain2	190.0	4140.0	1310.0	1320.0
timer fusion + subscription actuation	Chain1	140.0	2900.0	1470.0	1480.0
	Chain2	160.0	2890.0	1460.0	1470.0
timer fusion + timer actuation	Chain1	170.0	4730.0	2490.0	2500.0
	Chain2	190.0	4720.0	2480.0	2490.0

Table IV and Table V display the timing values of the system types for the over-utilized and under-utilized case, respectively. We further denote the sum of the execution times of the tasks along a chain as  $C_{chain}$  in Tables IV and V. For each chain, the  $C_{chain}$  column specifies the sum of its callback execution times. The upper bounds and lower bounds are derived based on the methods presented in Sections VI and VII-B, respectively. For the lower bound and observed values, the last callback of the actuator stores the timing values of both chains and are read out after the timing values remain static. In addition, the timing values of the lower bound and observed columns correspond to the maximum reaction time and the maximum data age, as we observed these values to be equal for every system and for all executions.

As shown in Table IV, the system types have different timing behaviors, with the subscription-based system having the best and the timer-based systems having the worst performance for the lower bound and observed values. The observed timing values of both chains are very similar and the lower bound of the simulated system is almost identical to the lower bound, but includes the overhead of running ROS2. For every system type, the upper bound exceeds the observed values by a large margin, as it assumes the worst-case execution pattern in every case. Additionally, the second chain that includes a passive subscription of a subscription fusion class has a very pessimistic upper bound compared to timer fusion classes. We could not observe a relation between the chain execution time and the timing behavior, as the chains directly effect each other when running on the same system.

Table V shows that an under-utilized system has a similar behavior, with timer-based systems performing worse than subscription-based ones. In addition, the margin between the upper bound and lower bound is much larger for each chain compared to the over-utilized system. This is due to the idle time of timer callbacks, which could result in large delays between message transfers. Similar to an over-utilized system, the observed values of an under-utilized system are close to the lower bound of the simulated system, and subscription fusion classes have a high upper bound for the second chain.

### IX. EVALUATION

As shown by the case study in Section VIII, the timing behavior of the under-utilized and over-utilized system is very different. In this evaluation, we further investigate this behavior and also determine the timing behavior of ROS2 systems when changing the number of components.

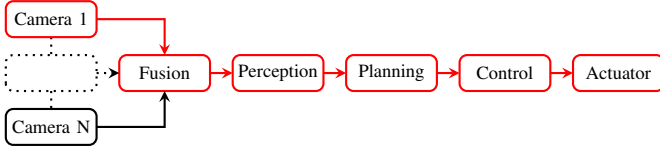


Fig. 6: Navigation system with variable number of cameras to evaluate the timing behavior of the chain highlighted in red.

In this section, we consider the basic autonomous driving system shown in Figure 6. It includes  $N$  cameras, a fusion, a perception, a planning, a control, and an actuator node. The cameras are sensor nodes, while the fusion node is implemented with a subscription fusion class. The actuator is a subscription actuator, while the perception, planning, and control nodes are implemented as filters. We determine the end-to-end timing latencies for the chain that is highlighted in red. It includes a static amount of callbacks, which include the sensor timer, one passive fusion subscription, one fusion timer, three filter subscriptions and one actuator subscriptions. We observe the timing behavior of this chain while changing the number of cameras of system. Each camera adds one sensor timer node and one passive fusion subscription to the system.

The system includes  $N$  cameras for each case. For the sensors, we use a timer with a period of  $100ms$  and a WCET of  $5ms$ . The sensor fusion includes one subscription per camera, each with a WCET of  $5ms$ . For each camera, the total WCET of the added callbacks, consisting of the the sensor node timer callback and fusion node passive subscription, is  $10ms$ . For the perception, the planning, the control, and the actuator subscriptions, the respective WCET is  $10ms$ . In total, the WCET of the filters and actuators is  $40ms$ . As a result, the system is under-utilized if the number of cameras is less than six, perfectly utilized if six cameras are included, and over-utilized if there are more than six cameras.

As shown in Figure 7, the timing behavior is very different for the under-utilized and over-utilized cases when changing the number of cameras. Over all cases, the upper bound is linearly increasing with the number of cameras, while the lower bound has two distinct patterns. If  $N \leq 5$ , the system is under-utilized and for each added camera an additional latency of  $10ms$  is added, which corresponds to the added WCET per camera, including the sensor timer callback and passive fusion subscription. For  $N = 6$ , the system is perfectly utilized and the observed lower bound is much smaller than the observed values. This can be explained by the overhead when running the system, which leads to the system being over-utilized and performing like an over-utilized system. For  $N \geq 7$ , the observed values and lower bound perform like an over-utilized system. In addition, the lower bound and observed values are very similar to the upper bound values for this chain. For the over-utilized chain, the timing value increases by  $70ms$  per added camera, as every callback is executed in every processing window and the chain consists of six callbacks and also needs to process the external event with one additional processing window.

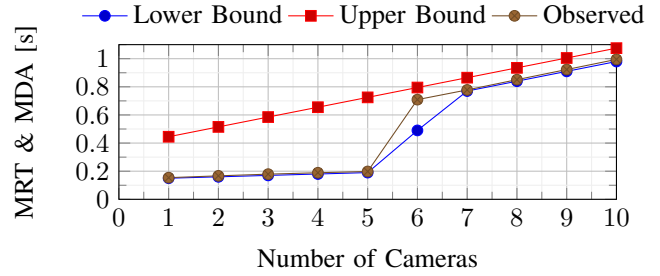


Fig. 7: End-to-end latencies of the system in Figure 6 when varying the number of cameras. The graphs show the values for both maximum reaction time and maximum data age, as these are equal for this system.

As shown in the evaluation, the under-utilized system performs much better than the over-utilized system. Therefore, it is important to consider the periods of all timers and the execution times of all callbacks that are registered to the executor. Additionally, we observe that our system does not leave the over-utilized case once it has reached it; hence, it is important that this state is never reached. For example, this can be done by guaranteeing that the sum of all execution times does not exceed the periods of each timer or by determining the execution patterns so that it does not transition to this state.

## X. CONCLUSION

In this paper, we explored the end-to-end timing analysis of ROS2 systems that are executed on a single ECU with a single-threaded executor. We introduce the main components that are part of the ROS2 architecture and form the systems. Based on these components, we introduce node classes, which specify the composition of these components and how they propagate data through the system. After that, we provide an upper bound analysis to determine the maximum end-to-end latencies of these systems. Additionally, we provide a simulation method to replicate the schedule when executing the system on a single executor. We introduce a measurement method to determine the end-to-end timing behavior when running ROS2 systems and when simulating the systems with our method.

The analysis shows that ROS2 systems perform vastly different depending on the utilization of the system. An under-utilized system performs much better than an over-utilized system and there is large margin between the observed values and the upper bound for the under-utilized case. In addition, ROS2 systems need to be guaranteed to never reach an over-utilized state, as they do not leave that state once it has been reached. The results demonstrate that the end-to-end analysis is an important aspect that needs to be considered when designing systems in ROS2. As the user can freely configure each system in ROS2, this analysis can provide insights on the expected end-to-end behavior for each configuration.

We plan to extend our analysis to systems that consist of multiple ECUs. Furthermore, we want to improve the scheduler design and provide guidelines for creating ROS2 systems that improve the general timing behavior.

## ACKNOWLEDGMENTS

This work has received funding by the German Federal Ministry of Education and Research (BMBF) in the course of the 6GEM research hub under grant number 16KISK038.

## REFERENCES

- [1] AUTOSAR. Specification of timing extensions, November 2020. release R20-11.
- [2] T. Blass, D. Casini, S. Bozhko, and B. B. Brandenburg. A ros 2 response-time analysis exploiting starvation freedom and execution-time variance. In *Proceedings of the 42nd Real-Time Systems Symposium (RTSS)*, 2021.
- [3] T. Blass, A. Hamann, R. Lange, D. Ziegenbein, and B. B. Brandenburg. Automatic latency management for ros 2: Benefits, challenges, and open problems. In *Proceedings of the 27th IEEE Real-Time and Embedded Technology and Applications Symposium (RTAS)*, 2021.
- [4] D. Casini, T. Blass, I. Lütkebohle, and B. B. Brandenburg. Response-time analysis of ros 2 processing chains under reservation-based scheduling. In *Proceedings of the 31st Euromicro Conference on Real-Time Systems (ECRTS)*, 2019.
- [5] H. Choi, Y. Xiang, and H. Kim. Picas: New design of priority-driven chain-aware scheduling for ROS2. In *27th IEEE Real-Time and Embedded Technology and Applications Symposium, RTAS 2021, Nashville, TN, USA, May 18-21, 2021*, pages 251–263. IEEE, 2021.
- [6] A. Davare, Q. Zhu, M. Di Natale, C. Pinello, S. Kanajan, and A. Sangiovanni-Vincentelli. Period optimization for hard real-time distributed automotive systems. In *Proceedings of the 44th Annual Design Automation Conference*, page 278–283, 2007.
- [7] M. Dürr, G. von der Brüggen, K.-H. Chen, and J.-J. Chen. End-to-end timing analysis of sporadic cause-effect chains in distributed systems. *ACM Trans. Embed. Comput. Syst.*, 18(5s), oct 2019.
- [8] N. Feiertag, K. Richter, J. E. Nordlander, and J. Å. Jönsson. A compositional framework for end-to-end path delay calculation of automotive systems under different path semantics. In *RTSS 2009*, 2008.
- [9] A. Girault, C. Prévot, S. Quinton, R. Henia, and N. Sordon. Improving and estimating the precision of bounds on the worst-case latency of task chains. *IEEE Transactions on Computer-Aided Design of Integrated Circuits and Systems*, 37(11):2578–2589, 2018.
- [10] M. Günzel, K. Chen, N. Ueter, G. von der Brüggen, M. Dürr, and J. Chen. Timing analysis of asynchronized distributed cause-effect chains. In *27th IEEE Real-Time and Embedded Technology and Applications Symposium, RTAS 2021, Nashville, TN, USA, May 18-21, 2021*, pages 40–52. IEEE, 2021.
- [11] S. Kato, S. Tokunaga, Y. Maruyama, S. Maeda, M. Hirabayashi, Y. Kit-sukawa, A. Monrroy, T. Ando, Y. Fujii, and T. Azumi. Autoware on board: Enabling autonomous vehicles with embedded systems. In *2018 ACM/IEEE 9th International Conference on Cyber-Physical Systems (ICCPs)*, pages 287–296, April 2018.
- [12] T. Kloda, A. Bertout, and Y. Sorel. Latency analysis for data chains of real-time periodic tasks. In *2018 IEEE 23rd International Conference on Emerging Technologies and Factory Automation (ETFA)*, volume 1, pages 360–367, 2018.
- [13] Open Robotics. Ros2: Foxy, May 2022. <https://docs.ros.org/en/foxy>.
- [14] G. Pardo-Castellote. Omg data-distribution service: architectural overview. In *23rd International Conference on Distributed Computing Systems Workshops, 2003. Proceedings.*, pages 200–206, 2003.
- [15] M. Quigley, K. Conley, B. Gerkey, J. Faust, T. Foote, J. Leibs, R. Wheeler, and A. Ng. Ros: an open-source robot operating system. volume 3, 01 2009.
- [16] Y. Saito, F. Sato, T. Azumi, S. Kato, and N. Nishio. Rosch:real-time scheduling framework for ros. In *2018 IEEE 24th International Conference on Embedded and Real-Time Computing Systems and Applications (RTCSA)*, pages 52–58, 2018.
- [17] J. Schlatow and R. Ernst. Response-time analysis for task chains in communicating threads. In *2016 IEEE Real-Time and Embedded Technology and Applications Symposium (RTAS)*, pages 1–10, 2016.
- [18] Y. Tang, Z. Feng, N. Guan, X. Jiang, M. Lv, Q. Deng, and W. Yi. Response time analysis and priority assignment of processing chains on ROS2 executors. In *41st IEEE Real-Time Systems Symposium, RTSS 2020, Houston, TX, USA, December 1-4, 2020*, pages 231–243. IEEE, 2020.
- [19] The Autoware Foundation. Autoware, 2022. <https://www.autoware.org/>.
- [20] H. Wei, Z. Shao, Z. Huang, R. Chen, Y. Guan, J. Tan, and Z. Shao. Rt-ros: A real-time ros architecture on multi-core processors. *Future Gener. Comput. Syst.*, 56:171–178, 2016.